

The Tunnel Sign Revisited: A Novel Observation of Cerebral Melioidosis Mimicking Sparganosis

Wee Ming Peh^{1,2*}, Goh Giap Hean³, Yong Hsiang Rong Clement^{1,4}

1. Department of Diagnostic Imaging, National University Hospital, Singapore

2. Department of Nuclear Medicine & Molecular Imaging, Singapore General Hospital, Singapore

3. Department of Pathology, National University of Singapore, Singapore

4. Yong Loo Lin School of Medicine, National University of Singapore, Singapore

* **Correspondence:** Wee Ming Peh, Department of Diagnostic Imaging, National University Hospital, 5 Lower Kent Ridge Road, Singapore 119074, Singapore

 Weeming.peh2@mohh.com.sg

Radiology Case. 2018 Aug; 12(8):1-11 :: DOI: 10.3941/jrcr.v12i8.3441

ABSTRACT

The tunnel sign has been described as a specific feature of cerebral sparganosis. We present a case of a 55-year-old gentleman found to have cerebral melioidosis and with initial imaging mimicking the appearance of sparganosis. This suggests that the tunnel sign in brain abscesses may be specific for infection by *Burkholderia Pseudomallei*, *Spirometra Mansoni* or *Listeria Monocytogenes*.

CASE REPORT

CASE REPORT

A 55-year-old gentleman of Southeast Asian descent presented at a routine gastroenterology outpatient appointment with a 1-day history of fever, chills and rigors. This was preceded by 1 week of headache, bilateral lower limb weakness and altered mental state in the form of increasing forgetfulness, incoherent speech and insomnia. He was previously involved in farm work. His past medical history includes type 2 diabetes mellitus (on glipizide, HbA1c 10%) as well as Child-Pugh score A liver cirrhosis secondary to chronic hepatitis C infection and alcohol use. The patient had also presented 2 months prior to colorectal surgery for a supralevator abscess and complex perianal fistula; the abscess was unable to be drained and he was treated conservatively with intravenous (IV) ceftriaxone and metronidazole that was subsequently converted to oral amoxicillin-clavulanate. He was subsequently admitted to hospital for investigation of his neurologic symptoms.

On examination, the vital signs were normal (blood pressure 121/72 mm Hg, pulse rate 80/minute, SpO₂ 100% on room air) and the patient was afebrile. Slow mentation was

noted although he remained oriented to time, place and person. His gait was unsteady, and power was reduced (grade 4- out of 5) in the bilateral lower limbs with associated hyper-reflexia. No signs of meningism were elicited. A perianal fistula was seen, covered with an iodine dressing, and this was clean. The rest of the physical examination was unremarkable.

The full blood count showed thrombocytopenia of 77 x 10⁹/L (normal range: 132-372 x 10⁹/L) but with no neutrophilia present. The C-Reactive protein levels were elevated at 17 mg/L (normal range: 0-10 mg/L). No other sources of sepsis were identified on chest radiography or urine formed element examination.

An unenhanced computed tomography (CT) scan of the brain was organized, which showed extensive right frontoparietal lobe edema with high-attenuation foci (Figure 1). An urgent contrast-enhanced magnetic resonance imaging (MRI) scan of the brain was subsequently performed, which showed a highly irregular, coalescing and rim-enhancing lesion in the right frontal lobe with tubular and linear components (Figures 2 to 5). Associated mass effect and restricted diffusion were present. There was adjacent pachymeningeal

enhancement as well as erosion of the inner table of the right frontal bone. The MRI findings suggested brain abscesses, although the on-call radiologist thought they were atypical for the usual pyogenic organisms and suggested the differential diagnosis of cerebral sparganosis based on the presence of the tunnel sign.

An urgent referral to neurosurgery was organized and the patient started on IV dexamethasone and anti-epileptics. A right frontal craniotomy was performed; intra-operatively, right frontal lobe brain abscesses were found, with pus and necrotic tissue seen in the abscess cavities. Histologic findings were compatible with a brain abscess (Figures 6 and 7). The visible abscesses were drained.

Cultures of the drained pus returned growth of *Burkholderia Pseudomallei*, sensitive to ceftazidime, cotrimoxazole and doxycycline. Apart from the known supraventricular abscess, no other thoracic or abdominal locus of infection was found on CT. Screen for cytomegalovirus, toxoplasma and human immunodeficiency virus was negative. The patient was reviewed by infectious disease specialists and started on a 6-week course of IV ceftazidime. The blood cultures were negative throughout the admission.

Dense left hemiplegia was noted in the immediate post-operative period, which improved with physiotherapy at the point of discharge 2 weeks later. However, 3 weeks after discharge, surveillance contrast-enhanced CT scan showed recurrent abscess in the surgical cavity (Figure 8). The patient was re-admitted for a re-open craniotomy and excision of the right frontal lobe abscess, with thick brown fluid drained intra-operatively. A 4-week course of IV meropenem and a 6-month course of oral cotrimoxazole were completed. At last review a year later, the patient had residual left-sided weakness (power 4+ of 5) and sleep disturbances but was otherwise well. MRI at this point showed complete resolution of the original abscesses with right frontal lobe encephalomalacia (Figure 9).

DISCUSSION

Etiology & Demographics:

The causative organism for Melioidosis is *Burkholderia Pseudomallei*, a gram-negative, aerobic and motile bacillus which has been described as having a “safety pin” appearance. The bacterium is able to withstand harsh environments and favors conditions with moist soils and pooled surface water [1–3].

Unsurprisingly, it is endemic in several tropical countries across Southeast Asia and Australia, with cases also reported in India, China, Brazil and Malawi [1,4]. The global incidence is estimated to be 165,000 cases per annum, although the disease is likely to be under-reported due to poor access to proper diagnostic techniques [4]. In Singapore alone, 550 cases were reported over a 10-year period, with spikes in incidence related to rainfall levels and the monsoon season [5]. High case-fatality rates in excess of 50% have traditionally been reported [4], although more recent case series have shown reductions to less than 10% possibly related to

improvements in diagnosis and management [6]. A male predilection has been described [1]. The disease is also more common in the 4th to 6th decade of life, with only 1/5 of all cases in Thailand occurring in children less than 14 years of age [2].

Routes of entry into the human body include skin abrasions, inhalation or aspiration. Several risk factors, both related to the environment and host, have been identified. These include a history of soil/water exposure (e.g. rice farmers in Thailand), diabetes mellitus, chronic renal/lung/granulomatous disease, alcoholism and steroid use [1,2].

Clinical & Imaging Features:

The clinical presentation is protean and dependent on the locus of infection. Pulmonary involvement is most commonly seen, with presentation as either a pneumonia or pleural effusion [1,6]. Other sites of involvement include the genitourinary (prostatic abscesses in particular), skin, bloodstream, musculoskeletal and neurological systems in descending order of prevalence. Of note, neurological involvement is noted in approximately 5% of cases [1].

Multiple case series and reports have been published on central nervous system melioidosis; a recent case series from China showed that patients commonly presented with fever, headache, seizures and motor weakness. Associated neutrophilia is often present [8].

Definitive microbiological diagnosis can be made by culturing and isolating the bacterium on Ashdown’s medium. Serological tests are poorly sensitive and specific, particularly in endemic areas that show high prevalence of seropositivity [1].

On imaging, cerebral melioidosis typically presents as a pyogenic abscess with either solitary or multifocal ring-enhancing lesions accompanied by surrounding vasogenic edema and mass effect, predominantly hypodense on CT. On MRI, these are typically T2 hyperintense, T1 hypointense and show restricted diffusion on diffusion weighted imaging (DWI) [8–16]. No published apparent diffusion coefficient (ADC) ranges are available. A variety of enhancement patterns and shapes are possible; the lesions may be cyst-like, linear, nodular and coalescing [8]. Spread conforming to white matter tracts and cranial nerve pathways has also been seen [11]. Rapidly progressive lesions may be a feature [8].

Associated extra-axial involvement may be demonstrated in the form of leptomeningeal enhancement, subdural empyema, epidural abscesses [13,15], calvarial/vertebral osteomyelitis or subgaleal abscesses [8,17]. Concomitant sinusitis has been reported in a Singaporean series [16]. Dural venous sinus thrombosis may also be present [8]. Outside of the head and neck, other abscesses may also be found in the lungs and abdominal viscera, particularly the prostate gland [6,18,19].

On magnetic resonance spectroscopy (MRS), the lesions are expected to appear similar to typical pyogenic abscesses,

with lipid (0.8-1.2 ppm), lactate (1.3 ppm) and amino acid (0.9 ppm) peaks and low N-acetyl-aspartate (NAA) and choline levels [20]. However, an atypical case of melioidosis has been reported [10] with lack of the aforementioned peaks and paradoxically increased choline-to-NAA ratio.

No studies featuring perfusion weighted imaging (PWI) findings have been reported, but the lesions are expected to show the absence of increased perfusion in the enhancing rim on the relative cerebral blood volume (rCBV) maps [20,21].

Treatment & Prognosis:

Melioidosis is a difficult infection to treat due to the bacterium's resistance to a wide-range of antibiotics, including aminoglycosides, penicillins and rifamycins. Ceftazidime-based regimens are most widely used in the intensive-phase. Eradication-phase regimens include the use of agents such as cotrimoxazole, chloramphenicol and amoxicillin-clavulanate [1,22].

Apart from the high mortality associated with cerebral melioidosis, significant morbidity post-event is also known. Of 12 patients in an Australian series, 3 patients died, 6 patients had residual weakness and only 3 patients made a full recovery [23]. Recurrent infections are possible; in a series of 540 patients with melioidosis of any site in Australia, a recurrence rate of 6% was found out of the 465 patients who survived the initial episode [6].

Differential Diagnoses:

The differential diagnosis of subcortical or deep white matter ring-enhancing lesions in the brain is well-known and wide-ranging, including gliomas, metastases, typical pyogenic abscesses and demyelinating disease [24]. However, to the best of our knowledge, tubular enhancement in a linear or curvilinear fashion – the tunnel sign – has not yet been described in these common pathologies. It was originally suggested to be a specific sign of cerebral sparganosis [25]. We have found that it may also be demonstrated in cerebral melioidosis, as this case illustrates, as well as in cerebral listeriosis [26]. We propose that the tunnel sign, if seen, may be a specific finding for these three etiologic agents. The distinguishing features of sparganosis and listeriosis are outlined below.

Sparganosis

This is a rare zoonotic disease caused by the larvae of the parasite *Spirometra Mansoni*. The disease is reported chiefly in East Asia and associated with a history of ingestion of raw meats (e.g. frog, snake, fish) or contact with contaminated water [27,28]. Treatment is by surgical excision of the worm or, less effectively, with antiparasitic agents such as praziquantel [29]. The clinical course may be acute or chronic [7] and may also be seen in children [30]. Peripheral eosinophilia may be found but this is not a common feature [30].

Imaging appearances depend partially on the chronicity of disease as well as on the live status of the parasite [31]. Acutely, perilesional edema may be present with corresponding CT hypodensity and T2 hyperintensity, similar

to the appearance of melioidosis and listeriosis. Apart from the tunnel sign mentioned above, beaded enhancement patterns and migration of the enhancement [7,30–33] may also be seen. The tunnel and migration signs are associated with live worms and portend a poorer prognosis [7].

It has also been reported that hyperdense components on unenhanced CT (HU 50-70) may correspond to a live parasite [33]. This finding is present in our presented case of cerebral melioidosis and cannot be used to distinguish the two.

Stigmata of chronicity may be present, which would not be seen in either *Burkholderia* or *Listeria* infections. For instance, punctate calcifications may be noted on CT, possibly representing degenerated larvae [31,33]. Cortical atrophy and ventricular dilatation may also be noted [30,33].

DWI iso-/hypointensity may be seen, in contradistinction with the restricted diffusion of melioidosis or listeriosis abscesses [32,34,35]. MRS may show slightly elevated choline and significantly decreased NAA levels, similar to that of neoplasms or granulomas [34,35]. PWI may show the absence of significantly increased perfusion to the lesion and to the surrounding tissue [35].

Listeriosis

Listeria Monocytogenes, a gram-positive non-spore-forming bacillus with a predilection for the intracellular space, is the offending agent. Brain abscesses are a rare manifestation, with only 56 cases reported from 1968 to 2011 [36]. Main risk factors for infection include ingestion of contaminated food and impaired host immunity. Treatment with ampicillin-based regimens is most commonly employed, with alternative options in trimethoprim-sulfamethoxazole, gentamicin, linezolid and rifampicin. Mortality rates of 40% have been reported with *Listeria* brain abscesses, similar to that of melioidosis [36].

The imaging findings of cerebral listeriosis are almost identical to that of melioidosis, presenting with the typical features of a pyogenic abscess [36]. Tubular enhancement patterns reminiscent of the tunnel sign have also been demonstrated [26,37–40] and diffusion tensor imaging (DTI) studies have shown that the lesions correspond to white matter fiber tracts [37,38]. MRS findings are also as expected for pyogenic abscesses [36].

It has been suggested that the extent of involvement in *Listeria* infections is less extensive compared to that of melioidosis [38]. Involvement of contiguous extra-axial structures in the form of subgaleal abscesses and calvarial osteomyelitis appears to be less commonly reported compared to cerebral melioidosis.

Pathological Considerations

The tunnel sign as originally described for cerebral sparganosis corresponds to the inflammatory reaction around the parasite in situ [25]. *Listeria Monocytogenes* has been shown to spread intra-axonally in in-vitro studies [41] and its linear pattern of spread along white matter tracts accounts for its worm-like appearance. Although no DTI studies have been

performed for cerebral melioidosis, the bacterium has been shown to travel along axon conduits [42,43] and is expected to mimic the patterns of spread of *Listeria*. To the best of our knowledge, such tunnel-like patterns of enhancement have yet to be reported in other neurotropic organisms such as *Herpesviridae* and *Borrelia*.

TEACHING POINT

Tubular enhancement in a linear or curvilinear pattern – the tunnel sign – is an unusual appearance of brain abscesses. Its presence may be specific for infection by one of three etiologic agents - *Burkholderia Pseudomallei*, *Spirometra Mansoni* or *Listeria Monocytogenes*.

REFERENCES

- Cheng AC, Currie BJ. Melioidosis: epidemiology, pathophysiology, and management. *Clinical microbiology reviews* 2005; 18:383–416. PMID: 15831829
- Wiersinga W, van der Poll T, White NJ, Day NP, Peacock SJ. Melioidosis: insights into the pathogenicity of *Burkholderia pseudomallei*. *Nature reviews Microbiology* 2006; 4:272–82. PMID: 16541135
- White N. Melioidosis. *The Lancet* 2003; 361:1715–1722. PMID: 12767750
- Limmathurotsakul D, Golding N, Dance DA, et al. Predicted global distribution of *Burkholderia pseudomallei* and burden of melioidosis. *Nature Microbiology* 2016; 1:15008. PMID: 26877885
- Liu X, Pang L, Sim SH, et al. Association of melioidosis incidence with rainfall and humidity, Singapore, 2003–2012. *Emerging infectious diseases* 2015; 21:159–62. PMID: 25531547
- Currie BJ, Ward L, Cheng AC. The Epidemiology and Clinical Spectrum of Melioidosis: 540 Cases from the 20 Year Darwin Prospective Study. *PLoS Neglected Tropical Diseases* 2010; 4:e900. PMID: 21152057
- Hong D, Xie H, Zhu M, Wan H, Xu R, Wu Y. Cerebral sparganosis in mainland Chinese patients. *Journal of clinical neuroscience : official journal of the Neurosurgical Society of Australasia* 2013; 20:1514–9. PMID: 23911107
- Zhan Y, Wu Y, Li Q, Yu A. Neuromelioidosis: a series of seven cases in Hainan province, China. *Journal of International Medical Research* 2016; 45:856–867. PMID: 28351287
- Yong S-S, Hassan S-A, Wong P-S, Yoong K-Y. A Rare Presentation of Central Nervous System Melioidosis. *OALib* 2017; 04:1–8. DOI: 10.4236/oalib.1103346
- Liang C-C, Chen S-Y, Chen T-Y, Chen S-T. Central Nervous System Melioidosis Mimics Malignancy: A Case Report and Literature Review. *World Neurosurgery* 2016; 89:732.e19–732.e23. PMID: 26882971
- Hsu C, Singh D, Kwan G, et al. Neuromelioidosis: Craniospinal MRI Findings in *Burkholderia pseudomallei* Infection. *Journal of neuroimaging : official journal of the American Society of Neuroimaging* 2016; 26:75–82. PMID: 26256582
- Arif MA, Abid MH, Renganathan R, Siddiqui KA. Central and peripheral nervous system involvement in neuromelioidosis. *BMJ Case Reports* 2015; 2015:bcr2015211001. PMID: 26494715
- Saravu K, Kadavigere R, Shastry A, Pai R, Mukhopadhyay C. Neurologic melioidosis presented as encephalomyelitis and subdural collection in two male labourers in India. *Journal of infection in developing countries* 2015; 9. PMID: 26623640
- Vestal ML, Wong EB, Milner DA, Gormley WB, Dunn IF. Cerebral melioidosis for the first time in the western hemisphere. *Journal of neurosurgery* 2013; 119:1591–1595. PMID: 23767895
- Muthusamy K, Waran V, Puthuchery SD. Spectra of central nervous system melioidosis. *Journal of Clinical Neuroscience* 2007; 14:1213–1215. PMID: 17964168
- Chadwick DR, g, Sitoh YY, Lee CC. Cerebral melioidosis in Singapore: a review of five cases. *Transactions of the Royal Society of Tropical Medicine and Hygiene* 2002; 96:72–76. PMID: 11926000
- Kuan Y, How S, Ng T, Fauzi A. The man with the boggy head: cranial melioidosis. *Singapore medical journal* 2010; 51:e43-5. PMID: 20358143
- Kung C-T, Li C-J, Ko S-F, Lee C-H. A Melioidosis Patient Presenting with Brainstem Signs in the Emergency Department. *The Journal of Emergency Medicine* 2013; 44:e9–e12. PMID: 22494598
- Muttarak M, Peh W, Euathrongchit J, et al. Spectrum of imaging findings in melioidosis. *The British Journal of Radiology* 2009; 82:514–521. PMID: 19098086
- Muccio CF, Caranci F, D'Arco F, et al. Magnetic resonance features of pyogenic brain abscesses and differential diagnosis using morphological and functional imaging studies: a pictorial essay. *Journal of neuroradiology Journal de neuroradiologie* 2014; 41:153–67. PMID: 24957685
- Holmes TM, Petrella JR, Provenzale JM. Distinction between cerebral abscesses and high-grade neoplasms by dynamic susceptibility contrast perfusion MRI. *AJR American journal of roentgenology* 2004; 183:1247–52. PMID: 15505287
- Fisher DA, Harris PN. Melioidosis: refining management of a tropical time bomb. *The Lancet* 2014; 383:762–764. PMID: 24284288

23. Currie BJ, Fisher DA, Howard DM, Burrow J. Neurological melioidosis. *Acta Tropica* 2000; 74:145–151. PMID: 10674643
24. Smirniotopoulos JG, Murphy FM, Rushing EJ, Rees JH, Schroeder JW. Patterns of Contrast Enhancement in the Brain and Meninges. *Radiographics* 2007; 27:525–551. PMID: 17374867
25. Song T, Wang W-SS, Zhou B-RR, et al. CT and MR characteristics of cerebral sparganosis. *AJNR American journal of neuroradiology* 2007; 28:1700–5. PMID: 17885230
26. Sakarunchai I, Saeheng S, Oearsakul T, Sanghan N. *Listeria monocytogenes* brain abscess on MR imaging mimicking the track of a migrating worm like a sparganum: A case report. *Interdisciplinary Neurosurgery* 2016; 5:9–11.
27. Moon W, Chang K, Cho S, et al. Cerebral sparganosis: MR imaging versus CT features. *Radiology* 1993; 188:751–7. PMID: 8351344
28. Presti A, Aguirre DT, Andrés P, Daoud L, Fortes J, Muñoz J. Cerebral sparganosis: case report and review of the European cases. *Acta neurochirurgica* 2015; 157:1339–43; discussion 1343. PMID: 26085111
29. Kim D, Paek S, Chang K-H, et al. Cerebral sparganosis: clinical manifestations, treatment, and outcome. *Journal of Neurosurgery* 1996; 85:1066–1071. PMID: 8929496
30. Yu Y, Shen J, Yuan Z, et al. Cerebral Sparganosis in Children: Epidemiologic and Radiologic Characteristics and Treatment Outcomes: A Report of 9 Cases. *World neurosurgery* 2016; 89:153–8. PMID: 26855309
31. Liao H, Li D, Zhou B, et al. Imaging characteristics of cerebral sparganosis with live worms. *Journal of neuroradiology Journal de neuroradiologie* 2016; 43:378–383. PMID: 27726888
32. Li Y-XX, Ramsahye H, Yin B, Zhang J, Geng D-YY, Zee C-SS. Migration: a notable feature of cerebral sparganosis on follow-up MR imaging. *AJNR American journal of neuroradiology* 2013; 34:327–33. PMID: 22859282
33. Kim M, Yu I, Chang K-H, et al. Cerebral Sparganosis: The Differential Features between Live and Degenerated Worms on CT and MR Images. *Journal of the Korean Society of Radiology* 2010; 63:1–7.
34. Bo G, Xuejian W. Neuroimaging and pathological findings in a child with cerebral sparganosis. Case report. *Journal of neurosurgery* 2006; 105:470–2. PMID: 17184080
35. Chiu C-HH, Chiou T-LL, Hsu Y-HH, Yen P-SS. MR spectroscopy and MR perfusion character of cerebral sparganosis: a case report. *The British journal of radiology* 2010; 83:e31-4. PMID: 20139254
36. Limmahakhun S, Chayakulkeeree M. *Listeria monocytogenes* brain abscess: two cases and review of the literature. *The Southeast Asian journal of tropical medicine and public health* 2013; 44:468–78. PMID: 24050079
37. Bojanowski MW, Seizeur R, Effendi K, Bourgouin P, Magro E, Letourneau-Guillon L. Spreading of multiple *Listeria monocytogenes* abscesses via central nervous system fiber tracts: case report. *Journal of neurosurgery* 2015; 123:1593–9. PMID: 26090836
38. Hsu CC, Singh D, Watkins TW, et al. Serial magnetic resonance imaging findings of intracerebral spread of *Listeria* utilising subcortical U-fibres and the extreme capsule. *The neuroradiology journal* 2016; 29:425–430. PMID: 27558992
39. Karlsson WK, Harboe Z, Roed C, et al. Early trigeminal nerve involvement in *Listeria monocytogenes* rhombencephalitis: case series and systematic review. *Journal of Neurology* 2017; 264:1875–1884. PMID: 28730571
40. Mano T, Saito M, Yoshizawa T. Axonal invasion of *Listeria monocytogenes*: Implications for early diagnosis with magnetic resonance imaging. *Journal of the Neurological Sciences* 2017; 373:7–8. PMID: 28131231
41. Henke D, Rupp S, Gaschen V, et al. *Listeria monocytogenes* Spreads within the Brain by Actin-Based Intra-Axonal Migration. *Infection and Immunity* 2015; 83:2409–2419. PMID: 25824833
42. John JA, Ekberg JA, Dando SJ, et al. *Burkholderia pseudomallei* Penetrates the Brain via Destruction of the Olfactory and Trigeminal Nerves: Implications for the Pathogenesis of Neurological Melioidosis. *mBio* 2014; 5:e00025-14. PMID: 24736221
43. John JA, Walkden H, Nazareth L, et al. *Burkholderia pseudomallei* Rapidly Infects the Brain Stem and Spinal Cord via the Trigeminal Nerve after Intranasal Inoculation. *Infection and Immunity* 2016; 84:2681–2688. PMID: 27382023

FIGURES

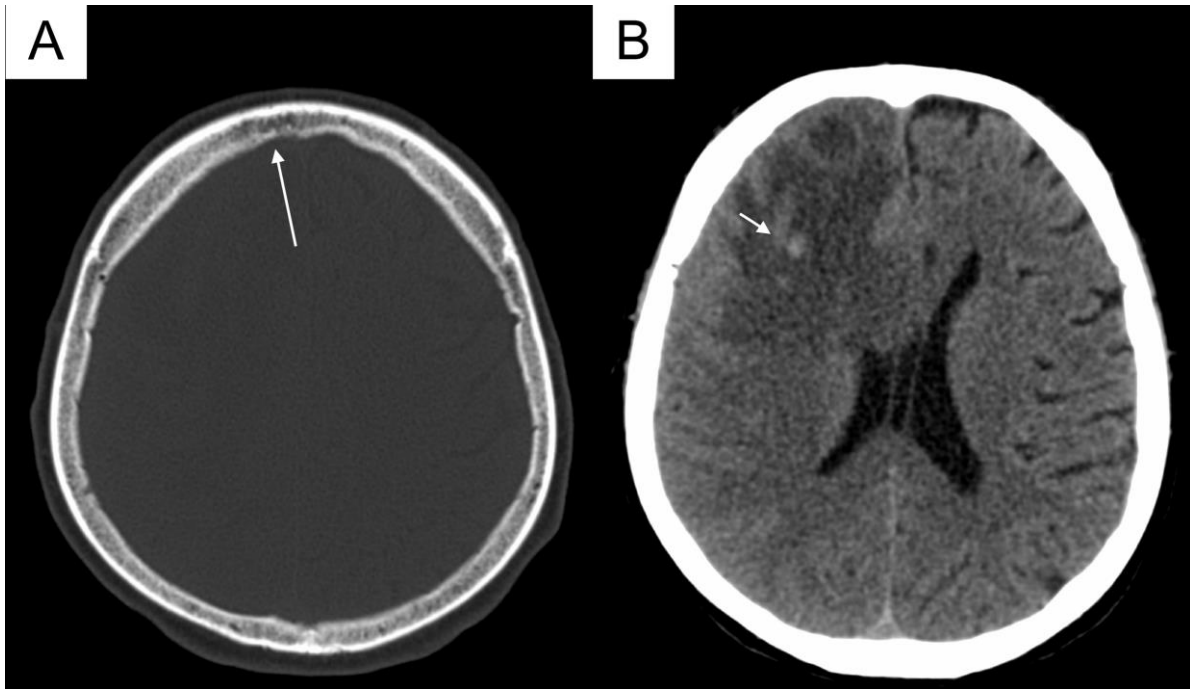


Figure 1: A 55-year-old gentleman with cerebral melioidosis

FINDINGS: A) Subtle erosion of the inner table of the right frontal bone is present (arrow) with associated lytic changes. B) On the initial CT, an ill-defined hypodensity is seen in the right frontal lobe with mass effect. Hyperdense foci are also seen within (HU 50, arrow, up to 0.7 x 0.5 cm in size), read as hemorrhagic stigmata, although this has been reported in sparganotic infections [33].

TECHNIQUE: Axial non-contrast CT, Siemens Sensation 64, 330 mAs, 120 kV, 3.00mm slice thickness

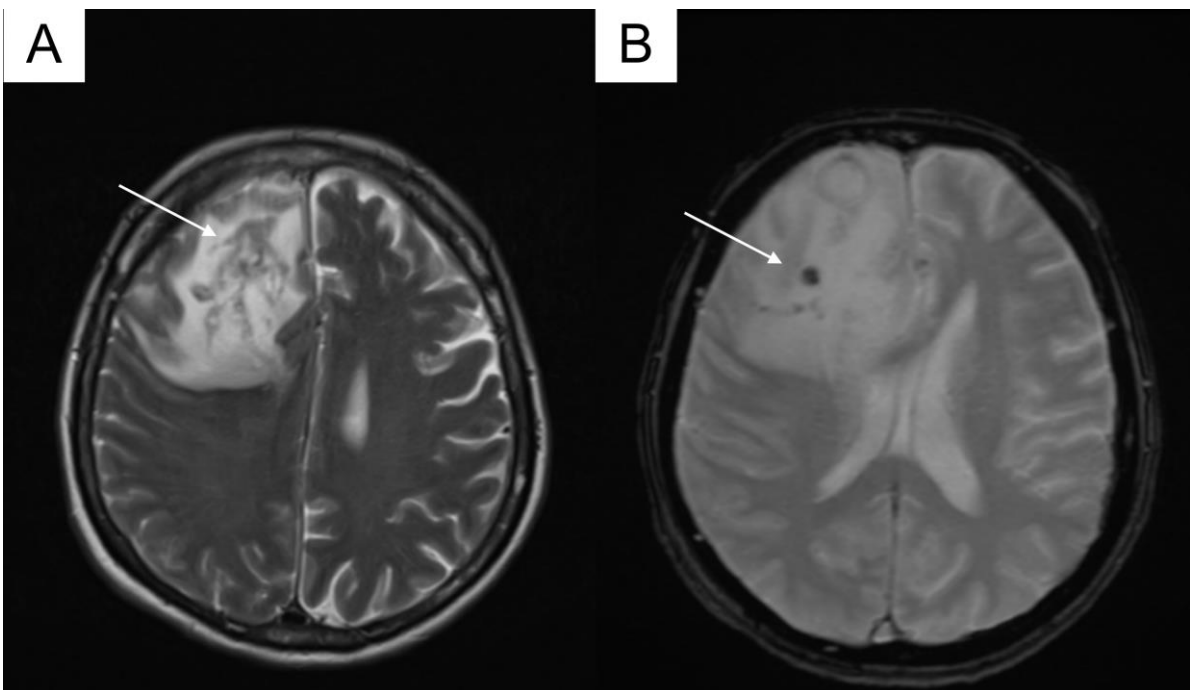


Figure 2: A 55-year-old gentleman with cerebral melioidosis

FINDINGS: A) T2-weighted axial MRI. An irregular lesion with predominantly central hyperintensity and peripheral iso-/hypointensity (arrow, up to 4.6 x 2.6 cm in axial dimensions) is noted, surrounded by extensive edema. B) Gradient recalled echo sequence (GRE) shows susceptibility foci (arrow, up to 0.5 x 0.5 cm in size) corresponding to the hyperdense areas on the previous CT, likely representing hemorrhage.

TECHNIQUE: Siemens Aera 1.5T. Ax T2: TE 112, TR 4380, 5 mm slice thickness, non-contrast. Ax GRE: TE 22, TR 629, 5 mm slice thickness, non-contrast.

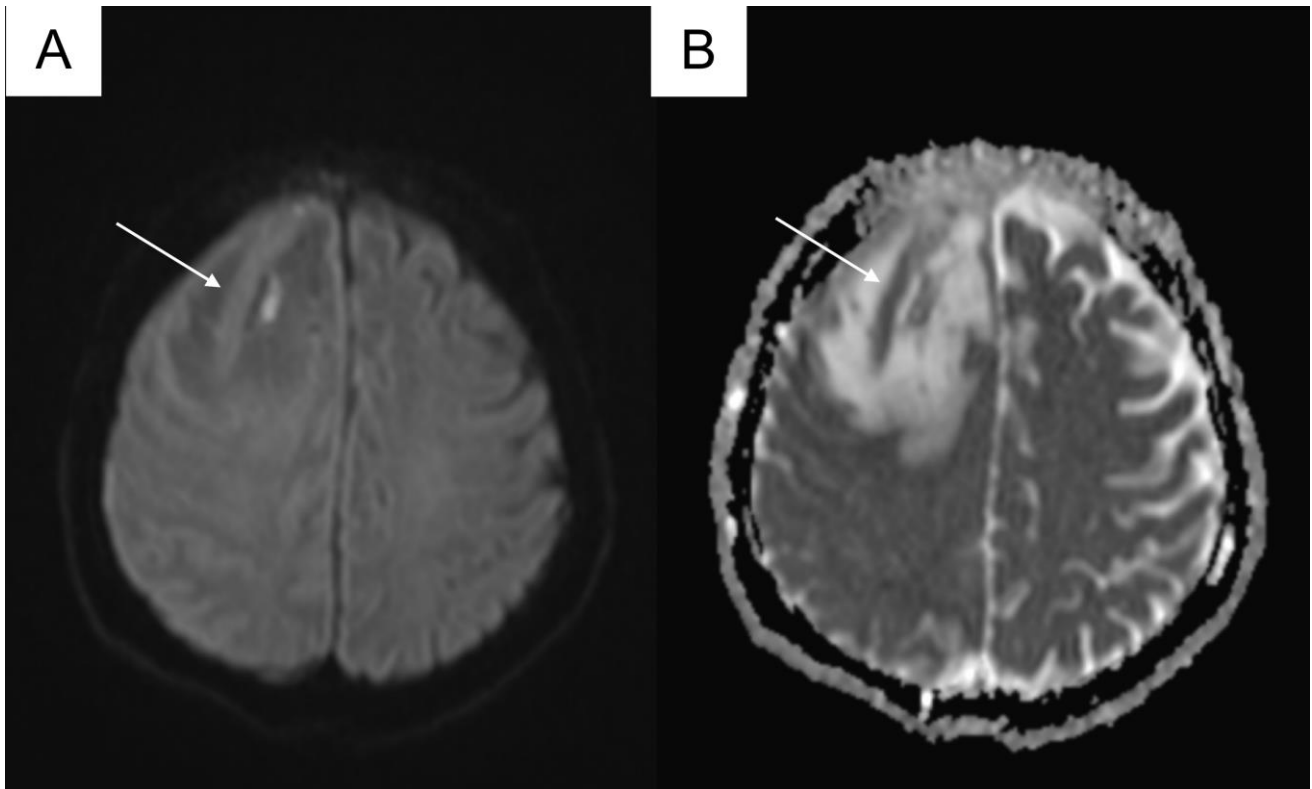


Figure 3: A 55-year-old gentleman with cerebral melioidosis

FINDINGS: A and B) DWI and corresponding ADC map. The core of the lesion shows features of restricted diffusion (arrows).
TECHNIQUE: Siemens Aera 1.5T. Ax DWI/ADC: TE 97, TR 4400, 5 mm slice thickness, B = 0/1000.

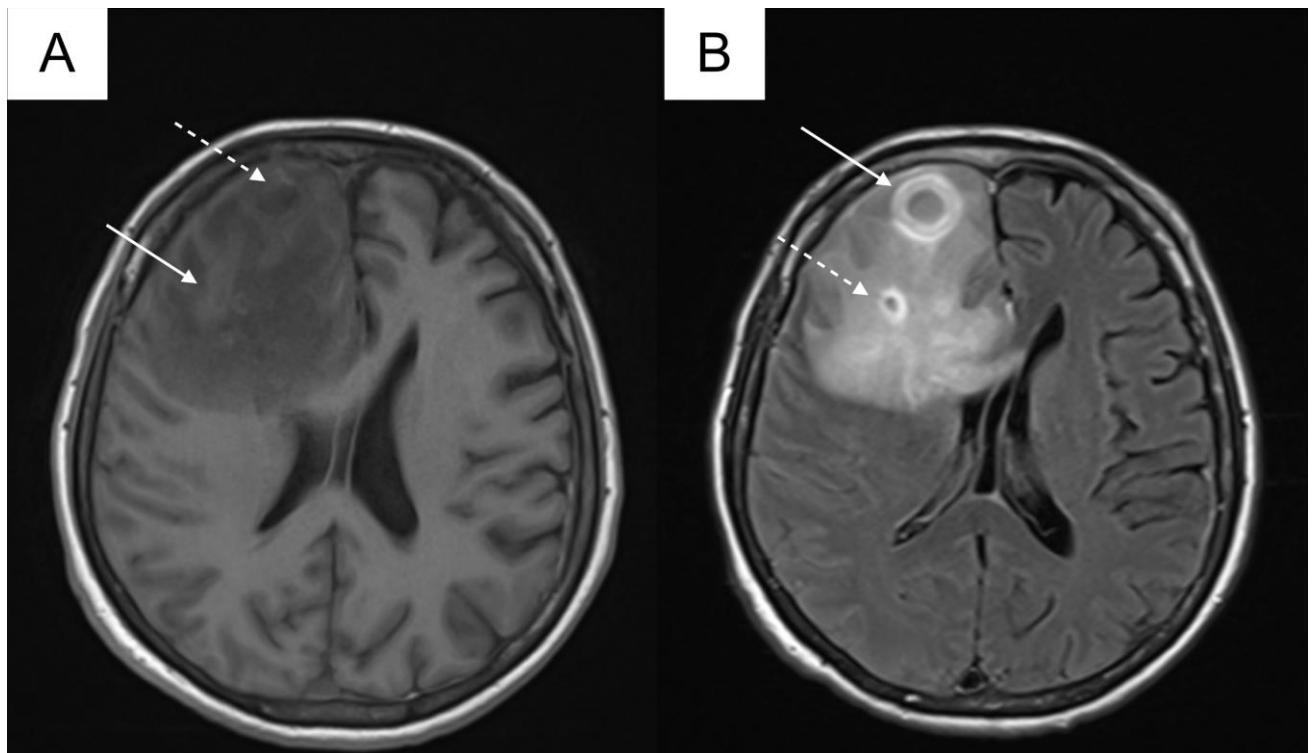


Figure 4: A 55-year-old gentleman with cerebral melioidosis

FINDINGS: A) Axial T1-weighted non-contrast. The lesion is predominantly hypointense (dashed arrow) with isointense components (solid arrow). B) Axial FLAIR post-contrast. A ring-enhancing cyst-like component is seen anteriorly (solid arrow, 2.1 x 1.9 cm) with perilesional edema. A smaller satellite lesion is also seen posteriorly (dashed arrow, 1.0 x 0.8 cm).
TECHNIQUE: Siemens Aera 1.5T. Ax VIBE: TE 4.77, TR 9.87, 3 mm slice thickness, non-contrast. Ax FLAIR +C: TE 84, TR 7000, 5 mm slice thickness, 14 mls gadoterate meglumine (Dotarem ®).

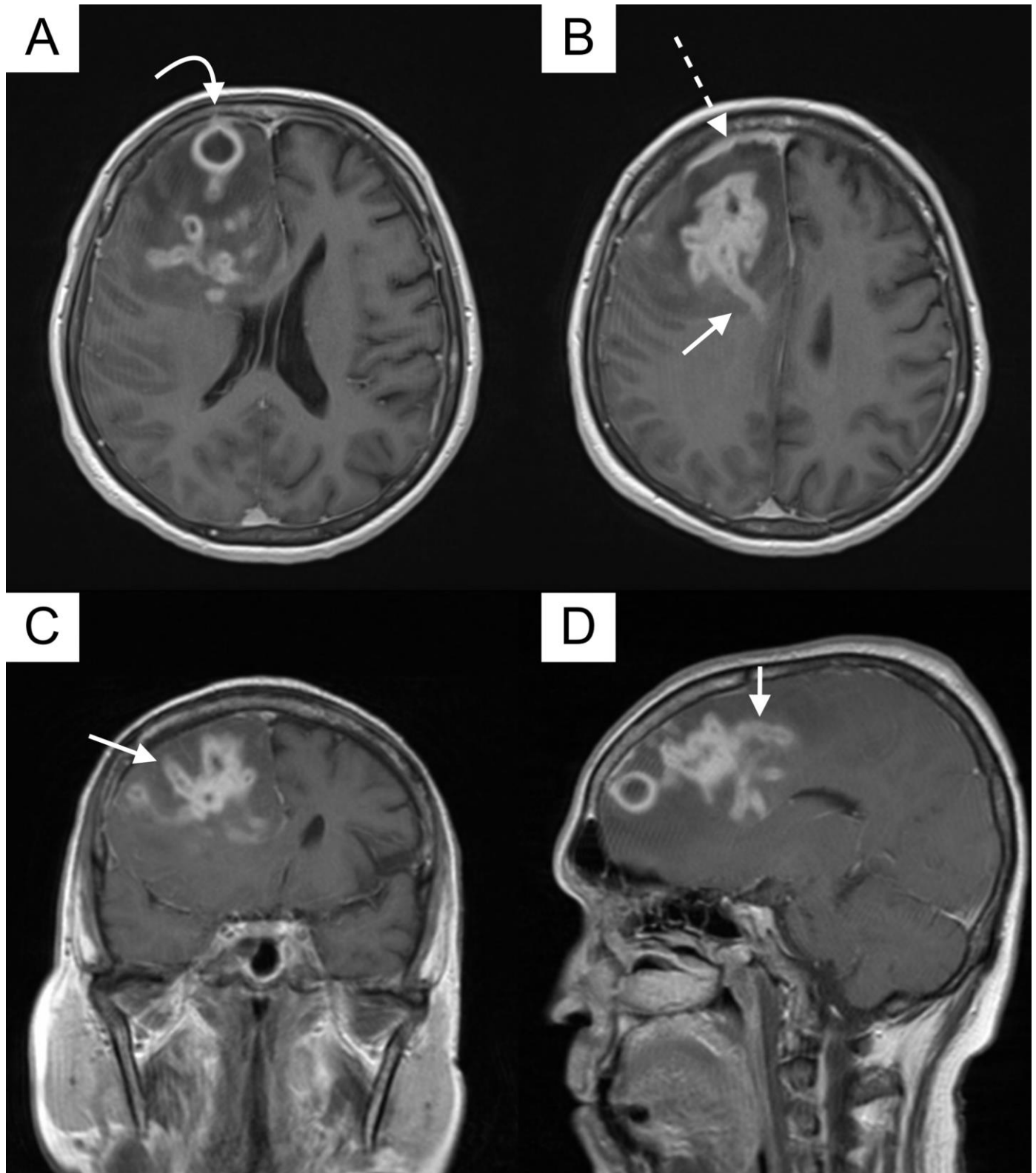


Figure 5: A 55-year-old gentleman with cerebral melioidosis

FINDINGS: Axial, coronal and sagittal post-contrast images showing a highly irregular, coalescing lesion with ring-enhancing as well as tubular, linear/curvilinear components, measuring up to 7.0 x 4.0 x 4.8 cm. Examples of the tunnel sign are shown (solid arrows). Anteriorly, there is associated pachymeningeal enhancement (dashed arrow) and involvement of the right frontal bone (curved arrow), suggesting contiguous spread of infection.

TECHNIQUE: Siemens Aera 1.5T. Ax VIBE+C: TE 4.77, TR 9.87, 3 mm slice thickness, 14 mls gadoterate meglumine (Dotarem®). Cor T1+C: TE 17, TR 663, 5 mm slice thickness, 14 mls gadoterate meglumine (Dotarem®). Sag T1+C: TE 17, TR 635, 5 mm slice thickness, 14 mls gadoterate meglumine (Dotarem®).

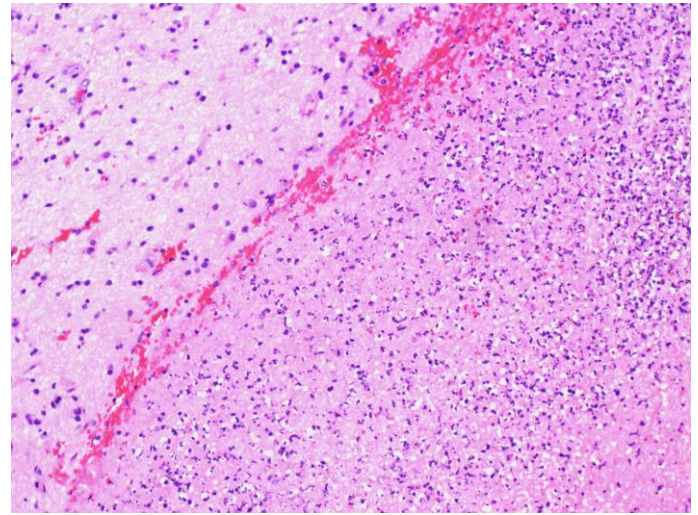
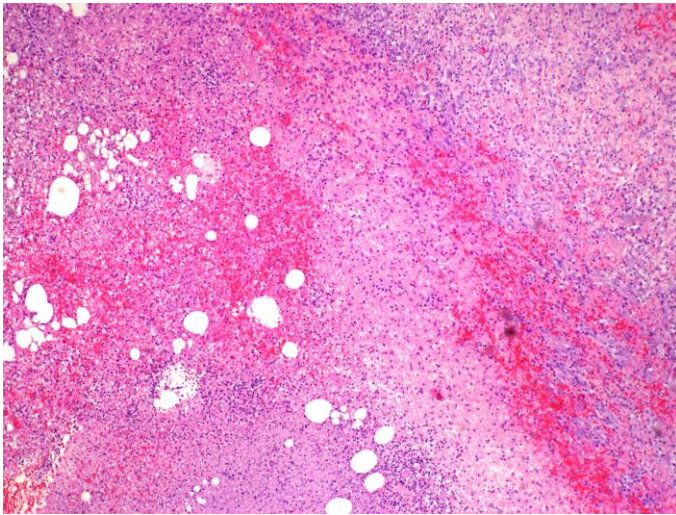


Figure 6: A 55-year-old gentleman with cerebral melioidosis
FINDINGS: Abscess with hemorrhage bordered by granulation tissue.
TECHNIQUE: Low-magnification photomicrograph (Hematoxylin & eosin stain; 40x)

Figure 7: A 55-year-old gentleman with cerebral melioidosis
FINDINGS: Abscess with adjacent gliotic brain parenchyma to the left.
TECHNIQUE: Intermediate-magnification photomicrograph (Hematoxylin & eosin stain; 100x)

Journal of Radiology Case Reports

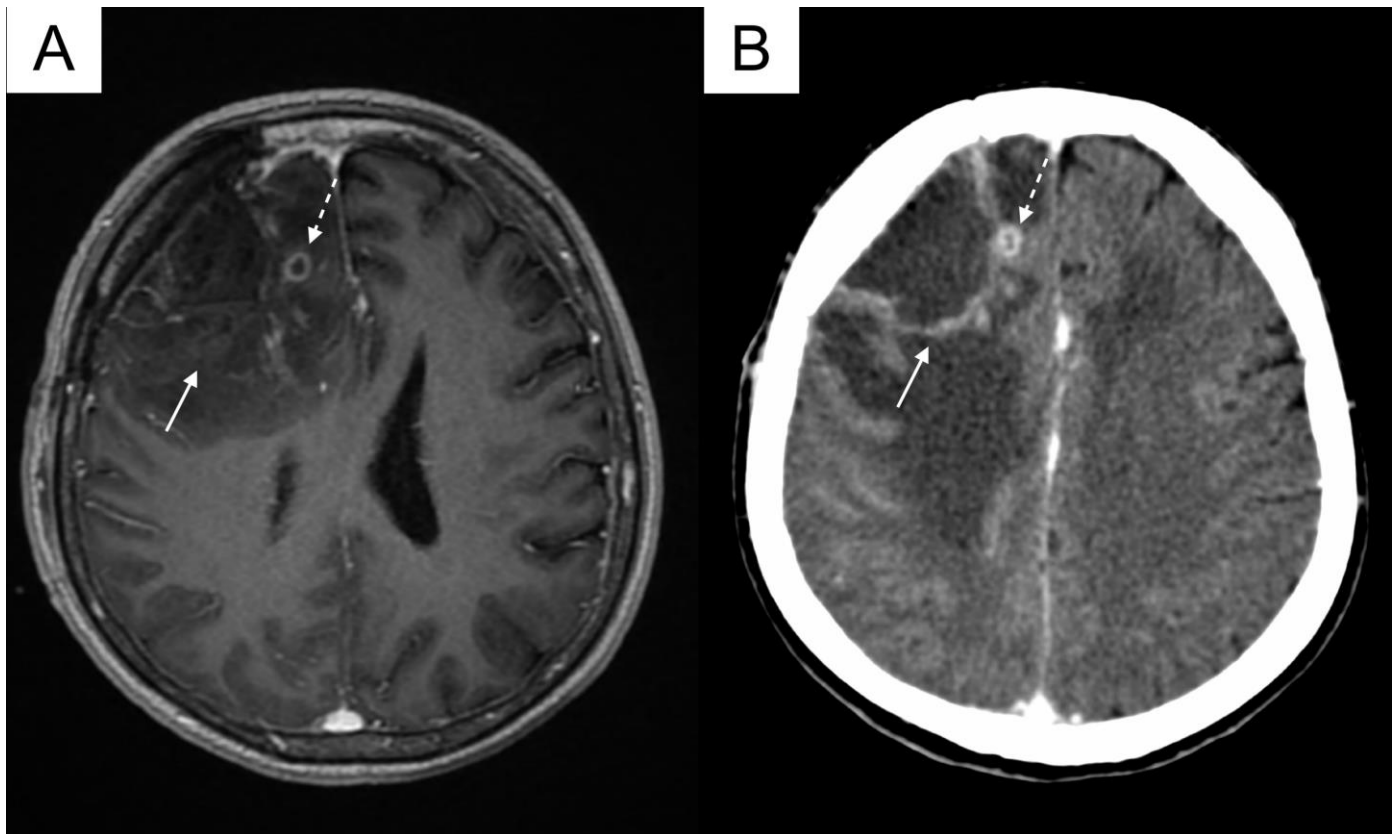


Figure 8: A 55-year-old gentleman with cerebral melioidosis
FINDINGS: A) Immediate post-operative MRI. This axial T1-weighted post-contrast image shows the surgical cavity with residual abscesses (dashed arrow). Note the absence of significant enhancement along the margins of the cavity (solid arrow). B) Contrast-enhanced CT 3 weeks after the initial admission now shows irregular enhancement along the margins of the surgical cavity (solid arrow, measuring up to 4.9 x 3.5 cm). This was proven to be a recurrent abscess on re-open craniotomy.
TECHNIQUE: 8a) GE Signa HDxt 1.5T. Ax 3D BRAVO Post contrast: TE 3.736, TR 9.504, 3 mm slice thickness, 15 ml gadoterate meglumine (Dotarem®). 8b) Axial post-contrast CT, Philips iCT 256, 300 mAs, 120 kV, 3.00mm slice thickness, Omnipaque 350 50 mls.

www.RadiologyCases.com

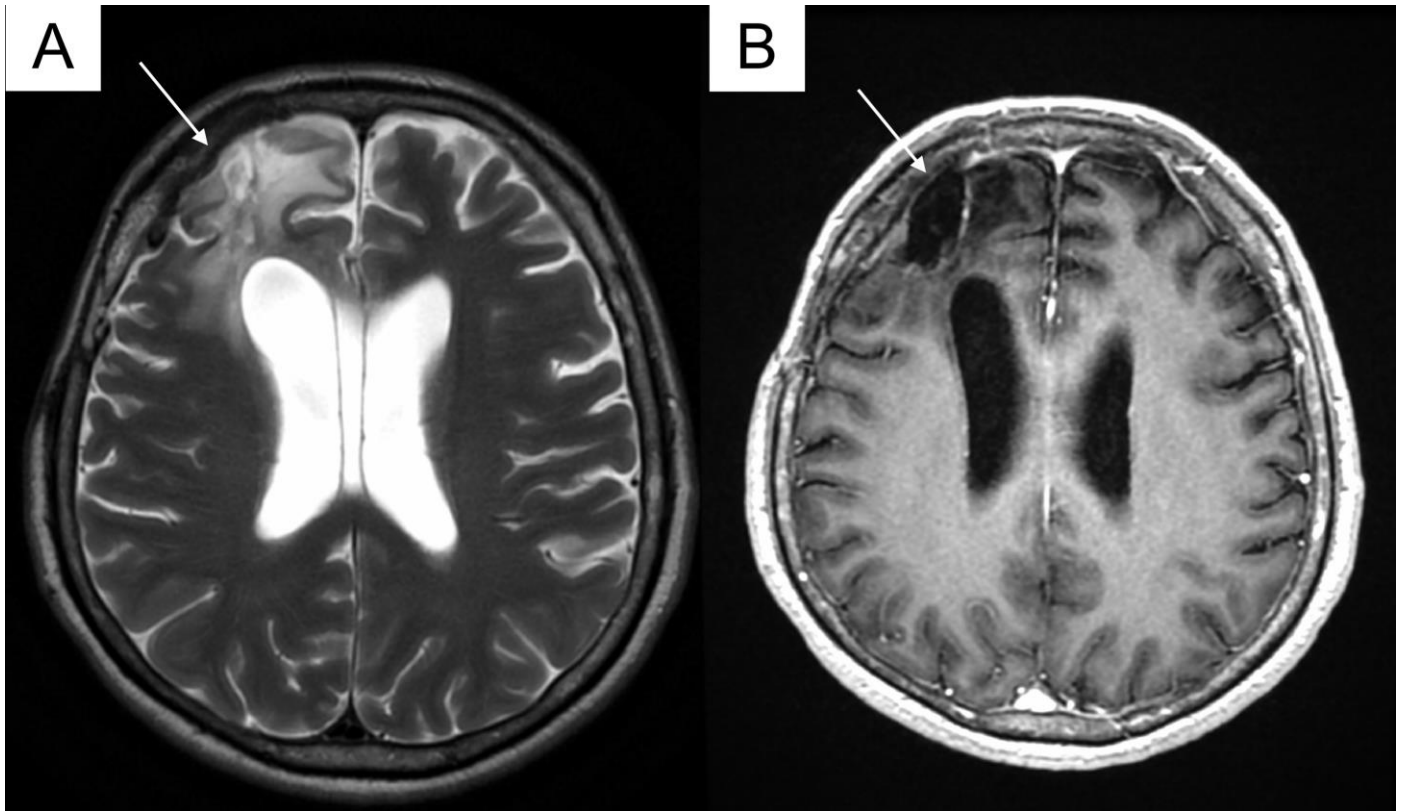


Figure 9: A 55-year-old gentleman with cerebral melioidosis

FINDINGS: MRI 1 year later. A) Axial T2-weighted image shows complete resolution of the abscesses and encephalomalacia of the right frontal lobe (arrow). B) Axial T1-weighted post-contrast image demonstrating resolution of the previously seen enhancing lesions.

TECHNIQUE: GE Optima MR450w 1.5T. Ax T2 FRFSE Prop: TE 112.896, TR 5250.74, 5 mm slice thickness, non-contrast. Ax T1 3D BRAVO+C: TE 4.804, TR 11.588, 3 mm slice thickness, 14 mls gadoterate meglumine (Dotarem®).

Etiology	Burkholderia Pseudomallei
Incidence	Globally – 165,000 cases per year (estimated) Cerebral melioidosis 5% of cases
Gender Ratio	More commonly in males
Age Predilection	Predominantly 4 th to 6 th decades of life
Risk Factors	Environment – wet seasons, soil/water exposure Host – diabetes mellitus, steroid use, chronic disease
Treatment	Ceftazidime-based antibiotic regimens
Prognosis	High mortality and morbidity rate Mortality rate as high as 50% previously
Findings on Imaging	<p><u>General features:</u></p> <ul style="list-style-type: none"> •Solitary/Multifocal •Ring-enhancing •Variety of shapes (e.g. cyst-like, linear, nodular, coalescing) •Rapidly progressive •Prominent extra-axial involvement <p><u>CT:</u></p> <ul style="list-style-type: none"> •Hypodense with mass effect <p><u>MRI:</u></p> <ul style="list-style-type: none"> •T2w: Hyperintense •T1w: Hypointense •DWI: Restricted diffusion •MRS: Similar to pyogenic abscesses (lipid, lactate and amino acid peaks)

Table 1: Summary of demographic and clinical features of melioidosis.

	Melioidosis	Sparganosis	Listeriosis
General Features/Contrast Enhancement Patterns	<ul style="list-style-type: none"> • Solitary/Multifocal • Ring-enhancing • Variety of shapes (e.g. cyst-like, linear, nodular, coalescing) • Rapidly progressive • Prominent extra-axial involvement 	<ul style="list-style-type: none"> • Similar to melioidosis • Migration of enhancement • Cortical atrophy and volume loss 	<ul style="list-style-type: none"> • Similar to melioidosis, but less prominent extra-axial involvement
CT	<ul style="list-style-type: none"> • Hypodense with mass effect 	<ul style="list-style-type: none"> • Hypodense with mass effect • May have hyperdense components • Punctate calcifications 	<ul style="list-style-type: none"> • Hypodense with mass effect
MRI (T1/T2/DWI)	<ul style="list-style-type: none"> • T2w: Hyperintense • T1w: Hypointense • DWI: Restricted diffusion 	<ul style="list-style-type: none"> • T2w: Hyperintense • T1w: Hypointense • DWI: Iso-/hypointensity 	<ul style="list-style-type: none"> • T2w: Hyperintense • T1w: Hypointense • DWI: Restricted diffusion
PWI	<ul style="list-style-type: none"> • Not reported. Likely to have normal rCBV in the enhancing rim 	<ul style="list-style-type: none"> • Normal rCBV in lesion and surrounding tissue 	<ul style="list-style-type: none"> • Not reported. Likely to have normal rCBV in the enhancing rim
MRS	<ul style="list-style-type: none"> • Similar to pyogenic abscesses (lipid, lactate and amino acid peaks) 	<ul style="list-style-type: none"> • Slightly elevated choline and decreased NAA 	<ul style="list-style-type: none"> • Similar to pyogenic abscesses (lipid, lactate and amino acid peaks)

Table 2: Differential diagnosis of cerebral melioidosis. *The key distinguishing features are highlighted in bold.*

ABBREVIATIONS

- ADC = apparent diffusion coefficient
- CT = computed tomography
- DWI = diffusion weighted imaging
- DTI = diffusion tensor imaging
- FLAIR = fluid attenuation inversion recovery
- FRFSE = fast recovery fast spin echo
- GRE = gradient recalled echo
- IV = intravenous
- L = liter
- MRI = magnetic resonance imaging
- MRS = magnetic resonance spectroscopy
- NAA = N-acetyl-aspartate
- PWI = perfusion weight imaging
- rCBV = relative cerebral blood volume
- VIBE = volumetric interpolated breath-hold examination

KEYWORDS

Tunnel Sign; Cerebral; Melioidosis; Sparganosis; Listeria; MRI

Online access

This publication is online available at:
www.radiologycases.com/index.php/radiologycases/article/view/3441

Peer discussion

Discuss this manuscript in our protected discussion forum at:
www.radiopolis.com/forums/JRCR

Interactivity

This publication is available as an interactive article with scroll, window/level, magnify and more features.
 Available online at www.RadiologyCases.com

Published by EduRad



www.EduRad.org